# Stochastic Uncertainty Quantification of the Conductivity in EEG Source Analysis by Using Polynomial Chaos Decomposition

Roman Gaignaire[1], Guillaume Crevecoeur[2], Luc Dupré[2], Ruth V. Sabariego[1], Patrick Dular[1,3], and Christophe Geuzaine[1]

[1]Department of Electrical Engineering and Computer Science (ACE), University of Liège, B-4000 Liège, Belgium
[2]Department of Electrical Energy, Systems and Automation, Ghent University, B-9000 Ghent, Belgium
[3]Fonds de la Recherche Scientifique, F.R.S.-FNRS, B-1000 Brussels, Belgium

**The electroencephalogram (EEG) is one of the techniques used for the non-invasive diagnosis of patients suffering from epilepsy. EEG source localization identifies the neural activity, starting from measured EEG. This numerical localization procedure has a resolution, which is difficult to determine due to uncertainties in the EEG forward models. More specifically, the conductivities of the brain and the skull in the head models are not precisely known. In this paper, we propose the use of a non-intrusive stochastic method based on a polynomial chaos decomposition for quantifying the possible errors introduced by the uncertain conductivities of the head tissues. The accuracy and computational advantages of this non-intrusive method for EEG source analysis is illustrated. Further, the method is validated by means of Monte Carlo simulations.**

***Index Terms*—Inverse problems, non-intrusive methods, polynomial chaos decomposition, stochastic methods.**

## I. Introduction

NEUROLOGICAL disorders, such as epilepsy, can be diagnosed by the use of the electroencephalogram (EEG). The EEG consists in measuring the potentials of a number of electrodes, typically 20 to 40, placed on the scalp of the patient over a period of time. These potentials are the result of electrical activity produced by the brain. The malfunctioning region in the brain must be accurately identified, especially in case of surgery. To this end, EEG measurements may be coupled to a numerical procedure in order to identify the neural sources in a so-called *EEG source analysis*. Two subproblems need thus to be solved: a forward and an inverse problem.

The EEG forward problem consists in simulating the EEG potentials for a given neural electrical activity. The following models need to be provided: 1) a head model incorporating the anatomical description and the characteristics of the different brain tissues; 2) a source model characterizing the brain activity from a physical and mathematical point of view. Solving the EEG inverse problem, the sources which correspond to the measured EEG potentials are determined. These sources can be identified with a good temporal resolution, contrary to other biomedical imaging techniques. The spatial resolution achieved is however low. The errors made when recovering the neural sources by means of a certain inverse numerical procedure must be quantified. In the head model, the geometry may give rise to errors that can be limited through e.g., the use of accurate Magnetic Resonance Images [1]. This is also applicable to errors made with respect to electrode positioning. Large uncertainties are still introduced with model parameters that are difficult to determine, e.g., the conductivity of the brain and the skull. The modelling error due to these unknown conductivities generates a spatial error, which can be significantly larger than the measurement noise. Determining the conductivities of the human tissues in the head is since years subject of research [2], [3]. Recently, a promising technique, based on magnetic resonance-electrical impedance tomography (MR-EIT) [4], was presented to determine these conductivities. From present and future measurements, a certain probability density function of the conductivities can be defined. Such a probability density function was also used in [5]. We propose to use so-called *non-intrusive probabilistic algorithms* to quantify the uncertainties on the location of the neural sources, which only assume the conductivity to be of finite variance [6], [7].

Manuscript received December 22, 2009; revised February 10, 2010; accepted February 16, 2010. Current version published July 21, 2010. Corresponding author: C. Geuzaine (e-mail: cgeuzaine@ulg.ac.be).

## II. Incorporation of Stochastic Uncertainty in EEG Source Analysis

### A. Definition of the Problem

The EEG forward problem starts from the location and orientation of neural sources, where the conductivities of the brain and the skull need to be provided, and calculates the EEG electrode potentials. For the sake of simplicity, we assume that the neural activity is represented by a single electrical dipole with a given location $\mathbf{r} = [r_x, r_y, r_z]^T$ and orientation $\mathbf{q} = [q_x, q_y, q_z]^T$. This is a widely spread approximation of the neural activity of patients suffering from epilepsy [8]. The brain to skull ratio of the conductivity $X$ is the important model parameter when solving the EEG forward problem. Since the proposed method accounts for the uncertainty on the conductivity without considering the error due to the geometrical model, we employ a coarse approximation of the head, i.e., a spherical head model. This model is a widely used approximation of the head consisting of three spheres that represent the brain (inner sphere), the skull (intermediate layer) and the scalp (outer layer); see Fig. 1(a). In this case a semi-analytical expression exists for the computation of the EEG potentials [9]. In our numerical tests we always use a standard configuration of $n = 27$ electrodes.

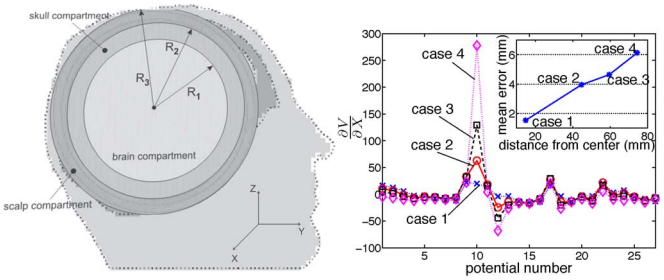


Fig. 1. (a) Three-shell spherical head model and (b) larger mean error for dipoles for which the potential is very sensitive to the conductivity.

The EEG forward model at a fixed time point is mathematically represented by

$$\mathbf{v} = \mathbf{L}(\mathbf{r})\mathbf{q} + \mathbf{e} \tag{1}$$

with measurement vector $\mathbf{v} \in \mathbb{R}^{n\times 1}$ and lead field matrix $\mathbf{L} \in \mathbb{R}^{n\times 3}$. This lead field or gain matrix comprises information from the geometry, the conductivities of the several tissues and the electrode positions. The error vector $\mathbf{e} = \mathbf{e}_n + \mathbf{e}_m \in \mathbb{R}^{n\times 1}$ comprises the electric noise $\mathbf{e}_n$ (due to the sensors and the background brain activity) and the modeling error $\mathbf{e}_m$. In this paper, we focus on the modelling error that is introduced due to the uncertain conductivity values in the head model. As widely accepted in practice, $\mathbf{e}_n$ is zero-mean Gaussian with known covariance matrix $\mathbf{C} = \mathrm{E}[\mathbf{e}\mathbf{e}^T] = \nu^2\mathbf{I}_n$ [10]. $\mathrm{E}[\cdot]$ denotes the expectation operator, $\nu$ is the noise variance and $\mathbf{I}_n$ is the $n$-dimensional identity matrix.

The EEG inverse problem searches the dipole parameter values $[\mathbf{r}^*, \mathbf{q}^*]$, given the electrode potential values $\mathbf{v}_{\mathrm{meas}}$ for a fixed electrode position. This is carried out by minimizing the EEG cost function [11]:

$$[\mathbf{r}^*, \mathbf{q}^*] = \arg\min_{[\mathbf{r},\mathbf{q}]\in\Omega} \frac{\|\mathbf{v}_{\mathrm{meas}} - \mathbf{L}(\mathbf{r})\mathbf{q}\|}{\|\mathbf{v}_{\mathrm{meas}}\|} \tag{2}$$

with $\Omega$ the search region. It is possible to express $\mathbf{v} = \mathbf{L}(\mathbf{r})\mathbf{q}$ as

$$\mathbf{v} = \mathbf{L}(\mathbf{r})\mathbf{L}^{\dagger}(\mathbf{r})\mathbf{v}_{\mathrm{meas}} \tag{3}$$

by using the optimal components in the least-squares sense $\mathbf{q}_{\mathrm{opt}}$, which can be found from the best approximated solution of the overdetermined system of linear equations $\mathbf{v} = \mathbf{L}(\mathbf{r})\mathbf{q}$:

$$\mathbf{q}_{\mathrm{opt}} = \mathbf{L}^{\dagger}(\mathbf{r})\mathbf{v}_{\mathrm{meas}}. \tag{4}$$

$\mathbf{L}^{\dagger}$ is the Moore–Penrose pseudo-inverse of the lead field matrix. In this way it is possible to redefine the inverse problem as

$$\mathbf{r}^* = \arg\min_{\mathbf{r}\in\Omega} \frac{\left\|\mathbf{v}_{\mathrm{meas}} - \mathbf{L}(\mathbf{r})\mathbf{L}^{\dagger}(\mathbf{r})\mathbf{v}_{\mathrm{meas}}\right\|}{\|\mathbf{v}_{\mathrm{meas}}\|} \tag{5}$$

with $\mathbf{q}^* = \mathbf{L}^{\dagger}(\mathbf{r}^*)\mathbf{v}_{\mathrm{meas}}$. This is a least-squares minimization problem, which can be solved using the Nelder–Mead simplex method; see, e.g., [11].

### *B. Non-Intrusive Method for EEG Source Analysis*

Spreading out the uncertainty from the conductivity to the position of the dipole is also an inverse problem. To solve this inverse problem we use the Nelder-Mead simplex method in combination with a non-intrusive stochastic approach based upon a chaos polynomial decomposition of both the conductivity and the dipole position [6]. The result of the inverse problem is thus a distribution of the dipole position.

Assuming that the conductivity ratio $X(\omega)$ is a random variable of finite variance defined in a probability space $(\Theta, F, P)$, it can be expanded as a truncated series of order $p_{\mathrm{in}}$ of Hermite polynomials $h_i$ of a random Gaussian variable $\xi(\omega)$, known as *Hermite chaos polynomials* [6]:

$$X(\omega) = \sum_{i=0}^{p_{\mathrm{in}}} X_i h_i\left(\xi(\omega)\right) \tag{6}$$

where $h_i$ is the polynomial of Hermite of order $i$ and $\omega$ is the random coordinate.

The inverse deterministic problem allows us to compute the position of the dipole given the value of the conductivity ratio $X$. When accounting for the uncertainty of the conductivity ratio $X(\omega)$ via (6) in the inverse problem, the output becomes a probabilistic distribution of the position of the dipole (no assumption made with regard to the shape of this distribution). This process can be seen as a "black box" where the dipole position in (5) is now given by $\mathbf{r}^* = \mathbf{r}(X(\xi(\omega)))$, i.e., a random vector $[r_x(\omega), r_y(\omega), r_z(\omega)]^T$ from the probability space $(\Theta, F, P)$ (where the conductivity ratio $X$ is also defined) to the sphere. Hence, the dipole position $\mathbf{r}_{\mathrm{NI}}$ belongs to a space that can be spanned by the polynomials $h_m(\xi(\omega))$, and can thus be written as a truncated series at an order $p_{\mathrm{out}}$:

$$\mathbf{r}_{\mathrm{NI}}(\omega) = \sum_{m=0}^{p_{\mathrm{out}}} \mathbf{r}_m h_m\left(\xi(\omega)\right). \tag{7}$$

The unknown real vector coefficients $\mathbf{r}_m$ are straightforwardly computed by applying the orthogonality properties of the Hermite polynomials, i.e.,

$$\mathbf{r}_m = \frac{E\left(\mathbf{r}_{\mathrm{NI}}(\omega) h_m\left(\xi(\omega)\right)\right)}{E\left(h_m\left(\xi(\omega)\right)^2\right)} \tag{8}$$

where $E(\cdot)$ is the mathematical expectation (note that the expectation of a vector is the vector of the expectations of its components). The denominator can be computed analytically. The integral in the numerator is calculated by means of a Hermite Gauss integration scheme with $d$ integration points [6]:

$$E\left(\mathbf{r}_{\mathrm{NI}}(\omega) h_m\left(\xi(\omega)\right)\right) \approx \sum_{i=1}^{d} w_i \mathbf{r}_{\mathrm{NI}}\left(X(t_i)\right) h_m(t_i) \tag{9}$$

where $t_i$ is the $i$-th Gauss point and $w_i$ the associated weight. The inverse deterministic problem is thus evaluated $d$ times with the conductivity ratio given by (6) and $\xi(\omega) = t_i, i = 1, \ldots, d$.

## III. Results and Discussion

We have performed computations using the Monte Carlo and the non-intrusive methods for several test cases corresponding to dipoles located increasingly farther from the center of the head (Cases 1 to 4 depicted in Fig. 1). In all four considered cases, the Monte Carlo simulations were carried out with a sample size of 50,000 (denoted $\mathbf{r}_{\mathrm{MC}}$). The accuracy of the non-intrusive approach is determined by three parameters: the order of the expansion of the input random variable $p_{\mathrm{in}}$ in polynomial chaoses, the order of the Hermite Gaussian integration scheme

$d$ in (9) and the order of the expansion of the polynomial random variable $p_{\text{out}}$. The effect of $p_{\text{in}}$ is not considered herein; a detailed study can be found in [6]. We have thus taken a fixed value $p_{\text{in}} = 13$. Different values are used for $d = 6, 8, 10$ and $p_{\text{out}} = 1, 3, 6$. The brain-to-skull conductivity ratio $X$ is chosen as a uniform random variable between 1/40 and 1/9. A fixed orientation ($y$-direction) of the dipole is assumed. Its location is given with regard to the center of the head model.

The non-intrusive approach presents several advantages with regard to other classical approaches such as the Cramer–Rao approximation [12] or the Monte Carlo method. The non-intrusive approach can handle a large set of probabilistic density functions with the only constraint of an input random variable with finite variance. Furthermore, an expansion of the output random variables is efficiently obtained. The Cramer–Rao bound is equally efficient but needs a Gaussian random variable as input and does not provide an expansion of the output, just a bound of the variance. The Monte Carlo method handles a large set of probabilistic density functions as well, but it is not time-efficient, e.g., a simulation with 50,000 samples normally distributed takes ~3 days while the non-intrusive approach requires less than 1 min (on a 2.26 GHz personal computer).

### A. Mean, Standard Deviation, and Covariance Matrix

We first compare global estimators such as the mean and the standard deviation obtained by the Monte Carlo (MC) and non-intrusive (NI) methods for the four different EEG data sets. Herein, the non-intrusive approach was applied with fixed $d = 10$ and $p_{\text{out}} = 6$.

The mean and the standard deviation of each coordinate of the dipole position are given in Tables I and II, respectively. Very good agreement between the results of the considered methods is observed for both estimators. In Table II, larger standard deviations are obtained for increasing distances from the center of the head. This means that the uncertainty on the spatial position of the source increases when it approaches the electrodes. In fact, the sensitivity of the potentials to the conductivity ratio is larger as the source is far from the center [Fig. 1(b)].

In order to prove that the inherent joint probability followed by $\mathbf{r}_{\text{NI}}$ converged to the one obtained by Monte Carlo, we compare the covariance matrices of $\mathbf{r}_{\text{NI}}$ for different $p_{\text{out}}$ to the covariance matrix of $\mathbf{r}_{\text{MC}}$ in Case 3.[1]

Let us define the relative difference in % between those matrices for the order $p_{\text{out}}$ as

$$\mathcal{D}_{p_{\text{out}}} = \left| \frac{\text{cov}\left(\mathbf{r}_{\text{NI}}(\omega)\right) - \text{cov}\left(\mathbf{r}_{\text{MC}}(\omega)\right)}{\text{cov}\left(\mathbf{r}_{\text{MC}}(\omega)\right)} \right| \cdot 100. \tag{10}$$

These matrices for $d = 10$ and $p_{\text{out}} = 1, 3$ and 6 are

$$\mathcal{D}_1 = \begin{bmatrix} 8.13 & 8.20 & 8.07 \\ 8.19 & 8.26 & 8.14 \\ 8.07 & 8.14 & 8.02 \end{bmatrix}, \quad \mathcal{D}_3 = \begin{bmatrix} 1.14 & 1.18 & 1.13 \\ 1.18 & 1.23 & 1.18 \\ 1.13 & 1.18 & 1.12 \end{bmatrix},$$

$$\mathcal{D}_6 = \begin{bmatrix} 0.36 & 0.34 & 0.36 \\ 0.34 & 0.32 & 0.34 \\ 0.36 & 0.34 & 0.35 \end{bmatrix}.$$

When increasing the order of the polynomial expansion of the output $p_{\text{out}}$, the covariance matrix of $\mathbf{r}_{\text{NI}}$ converges clearly to the covariance matrix of $\mathbf{r}_{\text{MC}}$. Indeed, for $p_{\text{out}} = 6$, the average difference is of 0.35% (see matrix $\mathcal{D}_6$).

[1] $\text{cov}(\mathbf{r}_{\text{NI}})(i,j) = (E((\mathbf{r}_{\text{NI}i} - E(\mathbf{r}_{\text{NI}i})(\mathbf{r}_{\text{NI}j} - E(\mathbf{r}_{\text{NI}j})))))_{1 \le i,j \le 3}$.

TABLE I
MEAN OF THE DIPOLE POSITION (mm)

| Case | Method | $\overline{r_x}$ | $\overline{r_y}$ | $\overline{r_z}$ |
|---|---|---|---|---|
| Case 1 | MC | 7.72 | 7.72 | 7.73 |
| | NI | 7.72 | 7.72 | 7.73 |
| Case 2 | MC | 23.54 | 23.34 | 23.65 |
| | NI | 23.52 | 23.32 | 23.64 |
| Case 3 | MC | 31.75 | 31.62 | 31.73 |
| | NI | 31.72 | 31.60 | 31.71 |
| Case 4 | MC | 39.49 | 40.07 | 39.33 |
| | NI | 39.46 | 40.03 | 39.31 |

TABLE II
STANDARD DEVIATION OF THE DIPOLE POSITION (mm) FROM THE CENTER OF THE HEAD IN THE $x$, $y$ AND $z$-DIRECTIONS

| Case | Method | $\sigma_{r_x}$ (mm) | $\sigma_{r_y}$ (mm) | $\sigma_{r_z}$ (mm) |
|---|---|---|---|---|
| Case 1 | MC | 0.53 | 0.53 | 0.53 |
| | NI | 0.54 | 0.54 | 0.53 |
| Case 2 | MC | 1.38 | 1.50 | 1.31 |
| | NI | 1.40 | 1.51 | 1.33 |
| Case 3 | MC | 1.63 | 1.70 | 1.64 |
| | NI | 1.65 | 1.72 | 1.66 |
| Case 4 | MC | 2.17 | 1.91 | 2.26 |
| | NI | 2.19 | 1.85 | 2.28 |

### B. Other Quantification and Convergence

From (7), it is easy and almost not time consuming to get a large sample of dipole positions with the non intrusive approach. All the classical statistical tools may thus serve not only to characterize the obtained samples (e.g., determine a cube bounding 95% of the locations) but also to study the convergence of the non-intrusive method results towards those of the Monte Carlo simulations.

A convergence analysis is performed for the non-intrusive approach by comparing the empirical cumulative functions and a density estimation of the output obtained by both methods with different values of $d = 6, 8, 10$ and $p_{\text{out}} = 1, 3, 6$.

Let us consider a sample of 50,000 values of positions. We can compute the empirical cumulative function $F(x) = P(X \le x)$ of the random variable $X$, i.e., the function which values at $x$ is the probability that the random variable $X$ takes a value less than or equal to $x$.

Fig. 2 shows the cumulative functions obtained with the Monte Carlo method and the non-intrusive approach with fixed $d = 10$ and $p_{\text{out}} = 1, 3$ and 6 in Case 1 along the $x$-direction. The cumulative functions of the non-intrusive method approach the Monte Carlo one when increasing $p_{\text{out}}$.

We compute then a probabilistic density estimation for both methods, i.e., we construct an estimate of the unobservable underlying probability density function linked to each sample. Fig. 3 depicts the density estimation for both methods in Case 3 along the $y$-direction. The curves of non-intrusive method (with $d = 10$ and $p_{\text{out}} = 1, 3$, and 6) converge clearly to the

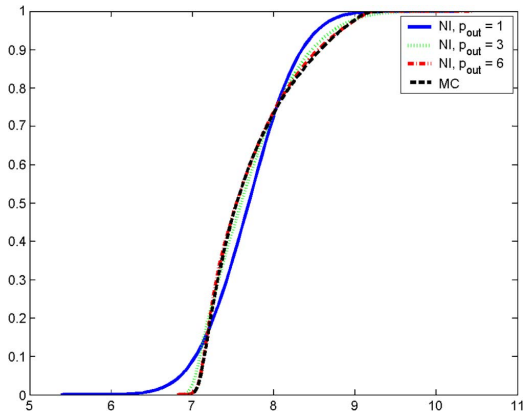


Fig. 2. Empirical cumulative function obtained with Monte Carlo and non-intrusive approaches in Case 1 along $x$-direction for fixed $d = 10$ and $p_{\text{out}} = 1, 3, 6$.

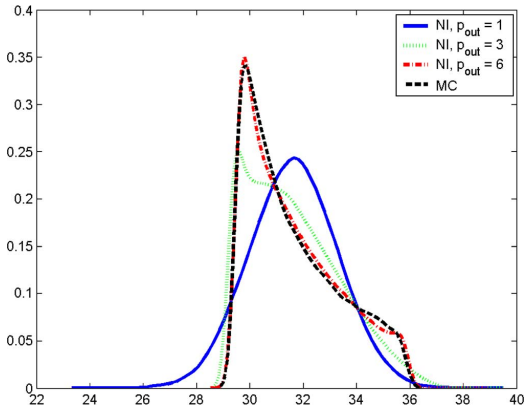


Fig. 3. Probabilistic density estimation obtained with Monte Carlo and non-intrusive approaches in Case 3 along $y$-direction for fixed $d = 10$ and $p_{\text{out}} = 1, 3, 6$.

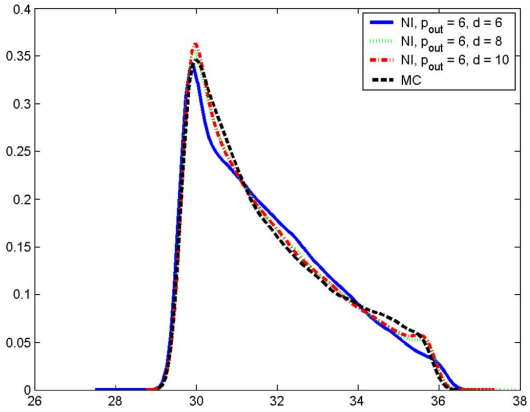


Fig. 4. Probabilistic density estimation obtained with the Monte Carlo and non-intrusive approaches in Case 3 along $z$-direction for fixed $p_{\text{out}} = 6$ and $d = 6, 8, 10$.

density estimation given by the Monte Carlo approach when $p_{\text{out}}$ increases.

A similar convergence behavior is evidenced when increasing the number of interpolation points $d$ for a fixed value $p_{\text{out}} = 6$. This convergence is illustrated in Fig. 4 for $d = 6, 8, 10$. The curves corresponding to $d = 8$ and $d = 10$ are really close to each other, what implies that the integration scheme has already converged and the addition of some points has a negligible effect on the improvement of the convergence. We may increase the value of $p_{\text{out}}$ instead.

## IV. Conclusion

A non-intrusive polynomial chaos decomposition approach has been proposed to take into account uncertainties in the EEG source analysis. The results have been validated by comparison to those given by the Monte Carlo method. Several statistical estimators have been considered and an excellent agreement observed. Furthermore, the non-intrusive stochastic approach has proved to be computationally efficiently with regard to the Monte Carlo method (less than 1 min versus 3 days). The presented non-intrusive approach can also furnish more information on the probabilistic dimension than other classical approaches such as the Cramer–Rao bound. Ongoing work concerns considering a real head model. The next step will be dealing with the EEG inverse problem tackling multiple dipoles.

## Acknowledgment

This work was supported by the Belgian Science Policy under grant IAP P6/21 and by the National Science Foundation under Grant DMS-0609824. G. Crevecoeur is a postdoctoral researcher of the FWO.

## References

[1] N. von Ellenrieder, C. H. Muravchik, and A. Nehorai, "Effects of geometric head model perturbations on the EEG forward and inverse problems," *IEEE Trans. Biomed. Eng.*, vol. 53, pp. 421–429, 2006.

[2] L. A. Geddes and L. E. Baker, "The specific resistance of biological material—A compendium of data for the biomedical engineer and physiologist," *Med. Biol. Eng.*, vol. 5, pp. 271–293, 1967.

[3] S. I. Gonçalves, J. C. de Munck, J. P. A. Verbunt, F. Bijma, R. M. Heethaar, and F. Lopes da Silva, "In vivo measurement of the brain and skull resistivities using an EIT-based method and realistic models for the head," *IEEE Trans. Biomed. Eng.*, vol. 50, no. 6, pp. 754–767, 2003.

[4] L. Özparlak and Y. Ider, "Induced current magnetic resonance—Electrical impedance tomography," *Physiolog. Measure.*, vol. 26, pp. 289–305, 2005.

[5] B. M. Radich and K. M. Buckley, "EEG dipole localization bounds and MAP algorithms for head models with parameter uncertainties," *IEEE Trans. Biomed. Eng.*, vol. 42, no. 3, pp. 233–241, 1995.

[6] R. Gaignaire, O. Moreau, B. Sudret, B. , and S. Clénet, "Propagation d'incertitudes en électromagnétisme statique par chaos polynomial et résolution non intrusive," presented at the NUMELEC'2006, Lille, France, Nov. 2006.

[7] R. Gaignaire, O. Moreau, B. Sudret, B. , and S. Clénet, "Current calculation in electrokinetics using a spectral stochastic finite element method," *IEEE Trans. Magn.*, vol. 4, pp. 754–757, 2008.

[8] J. de Munck, B. Van Dijk, and H. Spekreijse, "Mathematical dipoles are adequate to describe realistic generators of human brain activity," *IEEE Trans. Biomed. Eng.*, vol. BME-35, pp. 960–965, 1988.

[9] Y. Salu, L. Cohen, D. Rose, S. Sato, C. Kufta, and M. Hallett, "An improved method for localizing electric brain dipoles," *IEEE Trans. Biomed. Eng.*, vol. 37, pp. 699–705, 1990.

[10] C. H. Muravchik and A. Nehorai, "EEG/MEG error bounds for a static dipole source with a realistic head model," *IEEE Trans. Signal Process.*, vol. 49, pp. 470–484, 2001.

[11] B. Cuffin, "A method for localizing EEG sources in realistic head models," *IEEE Trans. Biomed. Eng.*, vol. 42, pp. 68–71, 1995.

[12] P. Stoica and A. Nehorai, "MUSIC, maximum likelihood, and Cramér-Rao bound," *IEEE Trans. Acoust., Speech, Signal Process.*, vol. 37, no. 5, pp. 720–741, 1989.